IL NUOVO CIMENTO **41 C** (2018) 116
DOI 10.1393/ncc/i2018-18116-6

COMMUNICATIONS: SIF Congress 2017

Protein-based nanocarriers for antimicrobial photodynamic therapy and subdiffraction localization of the theranostic agent

STEFANIA ABBRUZZETTI(*)

Dipartimento di Scienze Matematiche, Fisiche e Informatiche, Università degli Studi di Parma Parma, Italy

received 22 January 2018

Summary. — Nano-structures for photodynamical therapy can be assembled starting from a photosensitizer (PS) and a protein-based carrier, exploiting hydrophobic interactions. These chemical constructs preserve the PS photophysical and photosensitizing properties by preventing aggregation of non water-soluble PSs. This allows to obtain bio-compatible nanostructures that enhance the bio-availability of the PS. We demonstrate the interaction of Hypericin (Hyp), a naturally occurring PS that generates singlet oxygen with a high quantum yield, with two different proteins, apo-myoglobin and β-lactoglobulin. The constructs are highly effective against Gram-positive bacteria (*S. aureus* and *B. subtilis*). Interestingly, Hyp both free and bound to the protein can be exploited in super-resolution STED fluorescence microscopy, allowing for an accurate localization at cellular level of the PS and the photoinduced oxidation effects. Therefore, these structures show a double functionality, both therapeutic (based on photosensitization) and diagnostic (based on imaging), so that they can be considered *theranostic* agents. In conclusion, we demonstrate the potential of the protein-based nanostructures as water soluble and bio-compatible systems that can be relevant for applications in antimicrobial decontamination, both in clinical and in food and food-processing environment applications.

1. – Introduction

Recently, the term "theranostic" has been introduced in order to indicate an emerging research area in nano-medicine with the aim to develop chemical constructs that combine targeting, therapeutic and diagnostic functions within a single nanoscale complex [1]. "Classical" drug delivery systems, as liposomes, polymers, micelles, nanoparticles and antibodies have been loaded both with a drug and an agent for localization, exploiting photoluminescence of fluorophores or their properties as magnetic resonance constrast

(*) E-mail: stefania.abbruzzetti@unipr.it

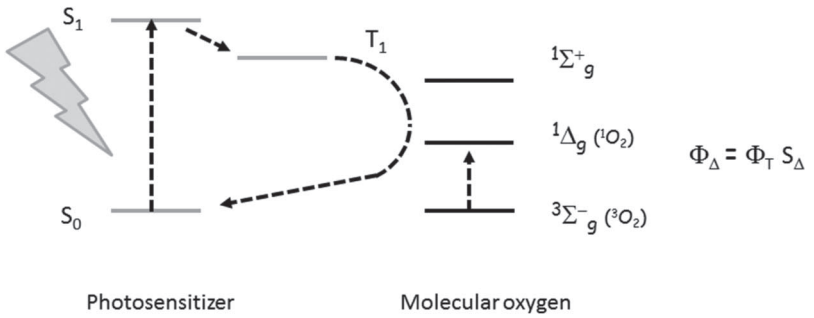

Fig. 1. – Simplified Jablonski diagram for the photosensitization of molecular oxygen. Non-radiative (inter-system crossing and quenching), and absorption transitions are indicated with black dashed arrows. S and T labels denote respectively singlet and triplet spin multiplicity of the PS.

agents [2]. Particularly interesting are the design and synthesis of nanoshell-based theranostic agents in order to improve the balance between efficacy and toxicity [3].

This theranostic approach can be considered for applications in photodynamic therapy (PDT) which is a clinically approved practice that can exert a selective cytotoxic activity toward malignant cells and pathogenic micro-organisms. PDT exploits the photodynamic effect, which implies the use of otherwise non toxic molecules, named photosensitizers (PSs), and visible light in the presence of molecular oxygen, to produce reactive oxygen species like free radicals or singlet oxygen, which result in cellular toxicity [4]. The oxidative damage or stress caused by the reactions with lipids, proteins or DNA are relevant and produce cellular death [5-7]. The essential photophysical features of the process are sketched in fig. 1.

In a photosensitization process, a PS is excited to an electronically excited state, usually a singlet state, by the absorption of a UV-visible photon and then with a significant probability undergoes an intersystem crossing transition to an excited triplet state (T_1). T_1 has a lifetime longer than the one of the excited singlet states and the correct spin multiplicity, that allows a photosensitized reaction with molecular oxygen. In fact, if T_1 has a suitable energy (at least 158 kJ/mol) an energy transfer process may occur: the PS returns to its initial singlet ground state while the molecular oxygen is simultaneously excited to an electronically excited singlet state (either $^1\Sigma_g^+$ or $^1\Delta_g$). The relaxation from $^1\Sigma_g^+$ to $^1\Delta_g$ is very fast in solution, therefore the final product of the reaction will always be the "singlet oxygen", simply indicated as $^1O_2$. The energy transfer process is called Dexter-type or electron-exchange mechanism, and consists in the simultaneous transfer of two excited electrons from one species to the other, so that there is no net charge transfer. The process is spin-allowed so it occurs with relatively high probability, but it requires a collision between the two partners since the wave functions of the involved electrons must overlap [8].

The effectiveness of a PS, measured by the $^1O_2$ photosensitization quantum yield Φ_Δ, can be expressed in general as

$$\Phi_\Delta = \Phi_T S_\Delta, \tag{1}$$

where Φ_T is the quantum yield for the triplet state formation and S_Δ the efficiency of the energy transfer process leading to $^1O_2$ generation.

It is evident that devising an effective photosensitizer implies first of all optimizing the photophysical parameters to maximize formation of productive states (high photosensitization quantum yield), but also assuring no dark toxicity and high molar extinction coefficient in the red/NIR spectral range to maximize the penetration in tissues and high bio-availability. This latter feature is closely related to the extent of the $^1O_2$ diffusion that can be estimated using the equation

$$d = (6D\tau)^{0.5}, \tag{2}$$

where d is the radial distance over a time τ and D is the diffusion coefficient. Considering the lifetime of $^1O_2$, a PS can produce an effective oxidative damage only if the photosensitization reaction is induced within about 100 nm from the target [9]. The issue is crucial for the applications because PSs are usually non soluble molecules, which in an aqueous solution form aggregates that quench the PS fluorescence emission and triplet state, preventing the production of $^1O_2$. Hence the requirement of finding vehicles able to bind the PS and transport it to the target, either a tumor cell or a bacterium.

Exploiting the fluorescence emission from PS molecules for imaging purposes turns the compound into a theranostic agent, being at the same time a pro-drug and a probe for imaging. This opens the opportunity for monitoring drug delivery, release and efficacy of these compounds, through direct visualization with fluorescence microscopy of the distribution of the drug and the damages induced upon illumination.

A key point remains the biocompatibility of the nanocarrier. To address this issue, we have recently proposed some proteins as natural candidates for transporting a hydrophobic drug such as a PS molecule. They offer important advantages related to the fact that a protein can be easily used and produced, selected to be biocompatible for applications in a particular environment, tailored to the target organism, and possibly engineered.

This approach can be considered not only for tumor PDT, but also for antimicrobial PDT (aPDT), originally developed in the '90s and now gaining growing interest for the treatment of localized infections [10,11]. Bacterial infections constitute a steadily growing problem in clinical practice, due to natural selection and misuse of antibiotics that lead to an increasing number of resistant bacteria, which renders the available drugs less effective or even useless. The recent report of the WHO, which predicts a post-antibiotic era in which minor infections or injuries may become a serious problem, underlines the demand of the development of novel antimicrobial treatment strategies [12]. Besides the increased prevalence of antimicrobial resistance, complex infection and immune evasion strategies of bacterial pathogens pose a serious threat for the affected patients and aPDT constitutes an important alternative treatment against resistant infections.

Moreover, the interest concerning aPDT has been recently extended beyond the clinical applications and one of the most promising is the decontamination of food and food-processing environment from common pathogen microorganisms (fungi, yeasts, molds and bacteria, often grown in bio-film). This is particularly important for not-cooked food like fruits, vegetables, sprouts, cheese and cold cuts. In these cases, an important issue is the biocompatibility of the photosensitizing agent, that must have low impact on the quality of the product [13, 14].

In the present paper, we summarize two examples of use of different protein scaffolds as bio-compatible nanocarriers for aPDT, loaded with a natural photosensitizer, Hypericin (Hyp), as reported in our recent papers [15-18]. We chose two proteins, wide-spread and

well-known representative of their respective families: apomyoglobin (apoMb), *i.e.* myoglobin without its physiological cofactor (heme), from horse heart, and β-lactoglobulin B (βLG), a dimeric protein belonging to the lipocalin family and the most abundant protein in the whey of cow milk. They can be both considered as carrier proteins, even if they are extremely different from several points of view like structure, origin, function and solvation properties.

2. – Materials and methods

The details concerning the preparation of samples, photoinactivation experiments, spectroscopic and imaging measurements have been thoroughly described in our previous works [15-18]. The only parameter determined in this work is the triplet quantum yield of Hyp bound to apoMb. It has been estimated from laser flash photolysis measurements using a comparative method with Hyp in dimethyl sulfoxide (DMSO) as a reference.

3. – Results and discussion

Hypericin (Hyp) is a naturally occurring PS, extracted from the plant *Hypericum perforatum* (St. John's wort), which has already proved to be efficient as an antibacterial [19] antiviral [20] and antifungal [21] photodynamic agent. The idea we are pursuing in these years is to design protein-based nanostructures for the delivery of Hyp as self-assembled, photophysically active supramolecular structures taking advantage of simple hydrophobic effect.

Hyp has a very similar chemical structure for size, shape hydrophobicity and symmetry to the heme and this fact suggests that it can form stable complex with apoMb. Indeed, computational modelling demonstrated that the hydrophobic cavity, which usually contains the heme in apoMb, can similarly host Hyp (fig. 2(A)). On the contrary, βLG shows a very different fold, typical of lipocalins, able only to accommodate linear hydrophobic molecules. However, forming dimers (2βLG) at its physiologically concentration [22], 2βLG is able to bind Hyp in correspondence to the clefts at the interface of the two monomers. In fact, as demonstrated by docking and MD simulations, a narrow cleft displays a larger affinity for Hyp and can accommodate the PS only as a monomer, whereas a wider cleft allows for the binding of dimeric PS molecules. In both cases, MD simulations show that slightly different orientations of PS within the pockets are possible (fig. 2(B)). It is important to note that if the self-assembling of the complex is a more complicated process for 2βLG than for apoMb, the interest of the lipocalin structure concerns the fact that more than one PS molecule can be transported and that 2βLG-Hyp can represent a bio-compatible system for antimicrobial decontamination in the dairy industry, considering that βLG is the most abundant protein in bovine milk whey [23].

Hyp is insoluble in water, while it is highly soluble in DMSO and ethanol. How can we demonstrate experimentally the formation of a self-assembled nanostructure between the protein (apoMb or 2βLG) that we want to use as a "vehicle" and Hyp as the "passenger" in aqueous PBS buffer? We can monitor spectroscopically this "vehicle-passenger" interaction by following the changes in the photophysical properties of Hyp. In fact, in DMSO and ethanol Hyp displays a well structured absorbance spectrum and an equally structured fluorescence emission spectrum, as shown in fig. 2(C). This emission is strongly reduced in PBS where Hyp forms aggregates and the bands in the absorbance spectrum

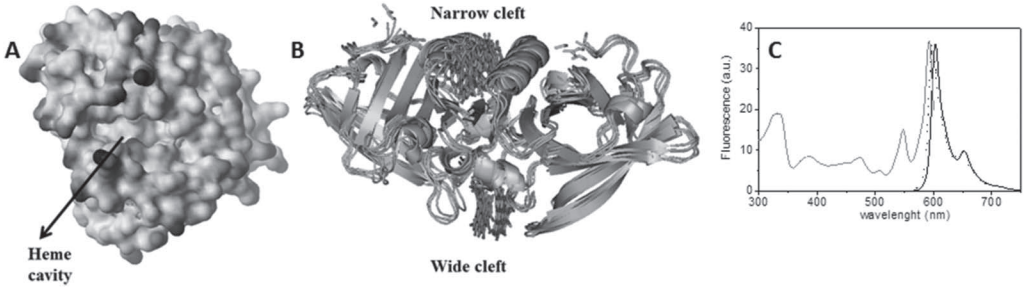

Fig. 2. – (A) Solvent-accessible surface of apoMb highlighting the heme-pocket suitable to bind Hyp. (B) The protein structure of 2βLG bound to Hyp molecules as monomers in the narrow cleft, and either monomers or dimers in the wide cleft. Hyp molecules are shown as sticks. (C) Fluorescence excitation spectrum of a 1 μM solution of Hyp in DMSO (gray solid line) and fluorescence emission spectra for Hyp in DMSO (black solid line), Hyp bound to apoMb (black dotted line) and in PBS buffer (black dashed line).

broaden. When a protein (apoMb or 2βLG) is added, Hyp recovers spectral features resembling those observed for monomeric Hyp dissolved in DMSO, *i.e.* sharper absorption bands and a more intense and structured fluorescence emission (fig. 2(C)). The recovery of spectral properties of monomeric Hyp is practically complete in apoMb-Hyp, whereas it is only partial in 2βLG-Hyp. This indicates that only in presence of apoMb a large fraction of Hyp molecules is not aggregated, it behaves as a monomeric species and is well solubilized by the interaction with the protein, where the PS senses a local environment with characteristics of polarity similar to those experienced in DMSO or ethanol. In other words, Hyp is accommodated in the hydrophobic cavity, vacated by removing the heme.

Further confirmations to complex formation come from steady-state fluorescence anisotropy (fig. 3(A)) and PS triplet state decay as monitored by triplet-triplet transient absorption (fig. 3(B)).

In fact, as can be observed in fig. 3(A), Hyp dissolved in DMSO shows zero anisotropy

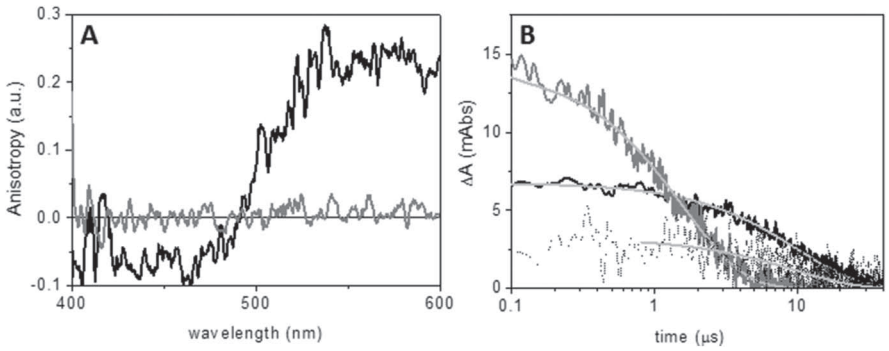

Fig. 3. – (A) Fluorescence steady-state anisotropy spectra of Hyp in DMSO (gray line) and apoMb-Hyp (black line) in PBS. (B) Triplet-triplet transient absorption kinetics of Hyp in DMSO (solid gray line), apoMb-Hyp (solid black line) and 2βLG-Hyp (dotted black line) in PBS. Fitting curves are superimposed to the experimental data (light gray lines). $T = 20\,^{\circ}$C. Adapted from ref. [18].

as a consequence of the rapid rotation of the molecule in solution which removes the initial orientation of the excited states dipole moment. Conversely, in the presence of apoMb, the anisotropy is non-zero meaning that Hyp rotation is much slower and the molecule holds a preferential orientation within its lifetime of fluorescence emission. This is a consequence of the interaction of Hyp with the cavity of apoMb, that induces constraints limiting the rotational diffusion of the molecule within its emission lifetime. Similar results are obtained for 2 βLG (data not shown).

Moreover, fig. 3(B) shows that the lifetime of triplet state of Hyp when apoMb or 2βLG are added becomes longer. This demonstrates that in apoMb-Hyp and 2βLG-Hyp the PS is protected from the environment and confirms the occurred self-assembling of the complexes.

The change in spectral properties of Hyp upon binding to the proteins provides a means to evaluate the affinity of the dye for the proteins. The value of the equilibrium constant for the formation of apoMb-Hyp and 2βLG-Hyp complexes is obtained by monitoring the fluorescence emission of Hyp at increasing concentration of the protein in PBS. Fitting the total fluorescence emission to the experimental data using eq. 1 reported in ref. [15], a value of $K_d = (4.2 \pm 0.8)\,\mu$M and $K_d = (0.71 \pm 0.03)\,\mu$M can be estimated for apoMb-Hyp and 2βLG-Hyp, respectively.

In order to use Hyp bound to a protein as a theranostic agent, two conditions should be verified. The first is that it is important that Hyp continues to be a fluorescence imaging probe, *i.e.* that its fluorescence quantum yield (Φ_F) remains to a significant level. Using a comparative method, where the emission of a molecule of known Φ_F is compared to the emission of the studied molecule, this parameter can be evaluated. The estimated value demonstrates that the emission properties of Hyp are preserved significantly when the PS forms a complex with apoMb ($\Phi_{\mathrm{F}} = 0.14 \pm 0.02$), and only partially when it is bound to 2βLG ($\Phi_F = 0.03 \pm 0.01$). The second question is: can the molecule sensitize $^1O_2$ to a respectable extent when it is bound in the cavity of a protein? In other words, does the PS continue to produce singlet oxygen? Production of reactive singlet oxygen can be demonstrated by observation of its specific phosphorescence at 1275 nm. From the time-resolved near-IR luminescence emission (1275 nm) by solutions of Hyp in DMSO, and the complexes of Hyp with the proteins in PBS, the lifetimes of the triplet state of PS and $^1O_2$ are obtained. Moreover, the quantum yield of $^1O_2$ photosensitization is readily calculated by comparison with a reference compound (Rose Bengal in PBS for apoMb-Hyp).

As a summary, photophysical properties of Hyp in DMSO and of the complexes are reported in table I. It has to be noted that 2βLG-Hyp has a smaller ability than free Hyp and apoMb-Hyp to emit fluorescence (lower Φ_{F}), excite the triplet state (lower Φ_{T}), and produce singlet oxygen (lower Φ_Δ). These results are the consequence of the fact that a fraction of Hyp is likely not fully monomeric and is embedded within an environment less polar than water, but not so much as in the hydrophobic heme cavity of apoMb. However, overall this characterization indicates that the shielding of Hyp from the solvent, due to the protein scaffold, does not preclude the formation of $^1O_2$, in particular for apoMb-Hyp, and demonstrates the potential of the protein-based nanostructures as water soluble and bio-compatible therapeutic agent for photosensitization-based applications.

As observed above, an accurate localization of the photosensitizing agent at the cellular level is extremely important for studying the effect of the photooxidation, since it reveals where the damage will be first induced. Conventional fluorescence microscopy is the easiest and more direct technique to image the distribution of a PS in a cell, but its resolution is limited by the diffraction of light to a few hundred nanometers. However,

TABLE I. – *Photophysical parameters of Hyp in DMSO, apoMb-Hyp and 2βLG-Hyp in PBS. The parameters for Hyp and apoMb-Hyp are from ref.* [18], *for 2βLG-Hyp from ref.* [17], *except where otherwise indicated.*

	Φ_F	τ_T (μs)	Φ_T	τ_Δ (μs)	Φ_Δ
Hyp	0.35 ± 0.02[24]	1.6 ± 0.1[a]	0.35[25]	5.5 ± 0.1	0.28 ± 0.05[b]
apoMb-Hyp	0.14 ± 0.02	11.6 ± 0.1	0.13 ± 0.04[a,c]	2.4 ± 0.4	0.14 ± 0.03
2βLG-Hyp	0.03 ± 0.01	10 ± 2	0.050 ± 0.002	2.3 ± 0.1	0.065 ± 0.010

[a] From Laser Flash Photolysis data.
[b] from NIR Phosphorescence data.
[c] Parameter determined in this work.

both free Hyp and Hyp bound to a protein based nanocarrier are amenable to be used as fluorescent reporters in super-resolution STED (Stimulated Emission Depletion) microscopy [26]. Figure 4 displays sample images of *Staphylococcus aureus* incubated with apoMb-Hyp and collected using confocal microscopy (panel (A)) and STED nanoscopy (panel (B)). Both images show that the cells become fluorescent after the incubation period and thus that the protein-based carrier delivered Hyp to the cells, preventing aggregation. However, the image undergoes a remarkable improvement in resolution when the STED beam is turned on. This allows to determine with higher precision the distri-

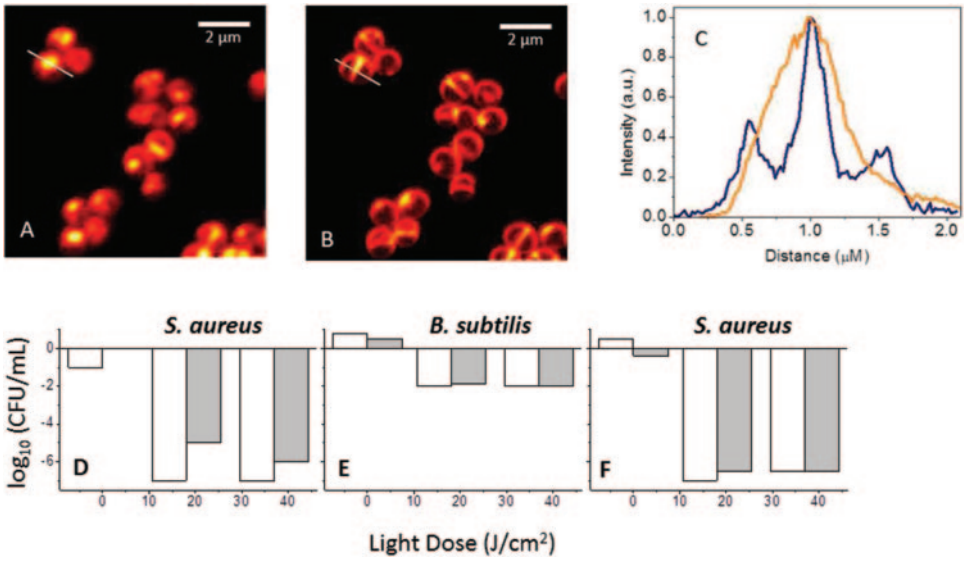

Fig. 4. – Comparison between *S. aureus* images collected with confocal microscopy (A) and with STED nanoscopy (B) after incubation with apoMb-Hyp. The gray and the black intensity profiles (C) were measured along the white segment in A and B, respectively. Images are collected under excitation at 566 nm and detection at 605–670 nm, with STED beam at 715 nm. Comparison between the light dose effects on photoinactivation of (D) Hyp and apoMb-Hyp on *S. aureus*, (E) Hyp and apoMb-Hyp on *B. subtilis* and (F) Hyp and 2βLG-Hyp on *S. aureus*. Hyp is in white and Hyp bound to the protein in gray. Adapted from ref. [18].

bution of the PS on bacterial cell wall, even if the improved resolution is not sufficient to determine the finer distribution of the PS on the components that constitute the cell wall, like the peptidoglycan layer or the membranes. The improvement in resolution can be better appreciated by inspection of the fluorescence emission profile along the cross section of a cell, as indicated in fig. 4(C). This reveals the accumulation of Hyp on an outer component of the cell, having a width in the order of 90 nm, compatible with the cell wall of the Gram-positive bacteria, and in areas connected to processes of cellular growth and division (not recognizable in the blurred confocal images, fig. 4 (A)).

Although a very similar distribution of Hyp (and complexes) on three bacterial types, belonging to Gram-positive (*Bacillus subtilis* and *S. aureus*) and Gram-negative (*E. coli*) class, the effect induced by irradiation on cells is remarkably different. The results of the photoinactivation experiments showing the bacterial cell viability after the phototreatment are summarized in fig. 4(D), 4(E), 4(F) and point out a major difference of efficacy between Gram-positive and Gram-negative bacteria. Considering apoMb-Hyp, the lower green light dose used ($18\,\mathrm{J\ cm^{-2}}$) is enough to decrease the number of colony forming units by 5 log units for *S. aureus*. Conversely, no sizeable effects are observed on the Gram-negative *E. coli*. The case of the Gram-positive *B. subtilis* appears intermediate, with an effect of light exposure inducing about a 2 orders of magnitude decrease in the number of bacterial colony forming units for both Hyp delivered with apoMb-Hyp and free Hyp. The different response of Gram-positive and Gram-negative bacteria to photosensitization-based treatment was reported in the literature for other PS molecules and has been correlated to the different structure of the bacterial cell wall [27], that is less permeable in the case of Gram-negative. Considering 2βLG-Hyp, the experiments were performed only on *S. aureus*, due to the relevance of infection by this bacterium in the dairy food chain, and demonstrate that the complex is able to inactivate *S. aureus* bacteria (about 5 logs).

Remarkably, in both cases (apoMb-Hyp and 2βLG-Hyp) the bacterial phototoxicity of complexes is not much different from that of free Hyp, but two major advantages of the use of PS loaded to a protein-nanocarrier can be identified. First, the dark toxicity appears lower for Hyp delivered with a protein than for free Hyp. Second, free Hyp must be dispensed as a concentrated solution in DMSO, which is decisively much less compatible with the use in clinical applications (apoMb-Hyp) or in food industry (2βLG-Hyp).

4. – Conclusion

We have demonstrated that the binding of a fluorescent PS, like Hyp, to a protein (apoMb and 2βLG) preserves the photophysical and photosensitizing properties of the active molecule. Therefore, the nanostructured system offers, in a single molecular species, a therapeutic functionality, based on photosensitization, and a diagnostic functionality based on fluorescence emission. These protein-based nanocarriers show the enormous advantage to be bio-compatible systems, that promote the solubilization of the PS, thus enhancing their photoactivity and increasing their bio-availability, fundamental features for application in the clinical practice and in food decontamination. The studied nanostructures demonstrate their significant efficacy on Gram-positive bacteria, but further studies related to a finer knowledge of PS distribution at cellular level may allow for a better comprehension of the different effect of aPDT on Gram-positive and Gram-negative bacteria.

* * *

I would like to thank Prof. Cristiano Viappiani for suggestions and discussions during the preparation of this manuscript. I am also grateful to all researchers that contributed to this project: Dr. Pietro Delcanale, Dr. Chiara Montali, Prof. Stefano Bruno at the University of Parma, Dr. Paolo Bianchini and Prof. Alberto Diaspro at the IIT in Genoa, Prof. Santi Nonell and Dr. Beatriz Rodriguez-Amigo of the Institut Quimic de Sarria in Barcelona, Prof. F. Javier Luque and Dr. Axel Bidon-Chanal of the Universitat de Barcelona. I am also grateful to Roberta Bedotti for her technical help. This research was partially funded by the Fondazione di Piacenza e Vigevano.

REFERENCES

[1] Bardhan R., Lal S., Joshi A. and Halas N. J., *Acc. Chem. Res.*, **44** (2011) 936.
[2] Caldorera-Moore M. E., Liechty W. B. and Peppas N. A., *Acc. Chem. Res.*, **44** (2011) 1061.
[3] Lammers T., Aime S., Hennink W. E., Storm G. and Kiesslig F., *Acc. Chem. Res.*, **44** (2011) 1029.
[4] Dolmans D. E. J.G. J., Fukumura D. and Jain R.K., *Nat. Rev. Cancer*, **3** (2003) 380.
[5] Cadet J., Douki T., Ravanat J. L. and Di Mascio P., in *Singlet Oxygen: Applications in Biosciences and Nanosciences*, edited by Nonell S. and Flors C. (Royal Society of Chemistry) 2016, pp. 393–407.
[6] Girotti A. W. and Korytowski W., in *Singlet Oxygen: Applications in Biosciences and Nanosciences*, edited by Nonell S. and Flors C. (Royal Society of Chemistry) 2016, pp. 409–430.
[7] Fudickar W. and Linker T., in *Singlet Oxygen: Applications in Biosciences and Nanosciences*, edited by Nonell S. and Flors C. (Royal Society of Chemistry) 2016, pp. 431–446.
[8] Michl J., in *Handbook of Photochemistry*, edited by Montalti M., Credi A., Prodi L. and Gandolfi M. T., III edition (CRC Press Taylor & Francis Group, Boca Raton) 2006, pp. 1–47.
[9] Ogilby R., *Chem. Soc. Rev.*, **39** (2010) 3181.
[10] Dai T., Huang Y.-Y. and Hamblin M. R., *Photodiagn. Photodyn. Ther.*, **6** (2009) 170.
[11] Kharkwal G. B., Sharma S. K., Huang Y. Y., Dai T. and Hamblin M. R., *Lasers Sur. Med.*, **43** (2011) 755.
[12] World Health Organization. *Antimicrobial Resistance: Global Report on Surveillance 2014* `http://www.who.int/drugresistance/documents/surveillancereport/en/` (2014).
[13] Luksiene Z. and Zukauskas A., *J. App. Microbiol.*, **107** (2009) 1415.
[14] Luksiene Z. and Brovko L., *Food Eng. Rev.*, **5** (2013) 185.
[15] Comas-Barcelò J., Rodríguez-Amigo B., Abbruzzetti S., del Rey-Puech P., Agut M., Nonell S. and Viappiani C., *RSC Advances*, **3** (2013) 17874.
[16] Rodríguez-Amigo B., Delcanale P., Rotger G., Juàrez-Jiménez J., Abbruzzetti S., Summer A., Agut M., Luque F. J., Nonell S. and Viappiani C., *J. Dairy Sci.*, **98** (2015) 89.
[17] Delcanale P., Rodríguez-Amigo B., Juàrez-Jiménez J., Luque F. J., Abbruzzetti S., Agut M., Nonell S. and Viappiani C., *J. Mat. Chem. B*, **5** (2017) 1633.
[18] Delcanale P., Pennacchietti F., Maestrini G., Rodríguez-Amigo B., Bianchini P., Diaspro A., Iagatti A., Patrizi B., Foggi P., Agut M., Nonell S., Abbruzzetti S. and Viappiani C., *Sci. Rep.*, **5** (2015) 15564.
[19] Kairyte K., Lapinskas S., Gudelis V. and Luksiene Z., *J. App. Microbiol.*, **112** (2012) 1144.

[20] Jacobson J. M., Feinman L., Liebes L., Ostrow N., Koslowski V., Tobia A., Cabana B. E., Lee D. H., Spritzler J. and Prince A. M., *Antimicrob. Agents Chemother.*, **45** (2001) 517.
[21] Rezusta A., López-Chicón P., Paz-Cristobal M. P., Alemany-Ribes M., Royo-Díez D., Agut M., Semino C., Nonell S., Revillo M. J., Aspiroz C. and Gilaberte Y., *Photochem. Photobiol.*, **88** (2012) 613.
[22] Mercadante D., Melton L. D., Norris G. E., Loo T. S., Williams M. A. K., Dobson R. C. J. and Jameson G. B., *Biophys. J.*, **103** (2012) 303.
[23] Kontopidis G., Holt C. and Sawyer L., *J. Dairy Sci.*, **87** (2015) 785.
[24] English D. S., Das K., Zenner J. M., Zhang W., Kraus G. A., Larock R. C. and Petrich J. W., *J. Phys. Chem. A*, **101** (1997) 3235.
[25] Darmanyan A., Burel L., Eloy D. and Jardon P., *J. Chim. Phys. Physicochim. Biol.*, **91** (1994) 1774.
[26] Hell S. W., *Science*, **316** (2007) 1153.
[27] Sperandio F. F., Huang, Y.-Y. and Hamblin M. R., *Recent Pat. Anti-infect. Drug Discov.*, **8** (2013) 1.